

Passivating Contact with Phosphorus-Doped Polycrystalline Silicon-Nitride with an Excellent Implied Open-Circuit Voltage of 745 mV and Its Application in 23.88% Efficiency TOPCon Solar Cells

Qing Yang, Zunke Liu, Yiran Lin, Wei Liu, Mingdun Liao, Mengmeng Feng, Yuyan Zhi, Jingming Zheng, Linna Lu, Dian Ma, Qingling Han, Hao Cheng, Zhenhai Yang, Kaining Ding, Weiyan Duan, Hui Chen, Yuming Wang, Yuheng Zeng,* Baojie Yan,* and Jichun Ye*

A P-doped polycrystalline silicon-nitride (n-poly-SiN_x) as the electron selective collection layer in a tunnel oxide passivated contact (TOPCon) solar cell is reported. The nitrogen content is controlled by the active gas ratio of $R = \text{NH}_3/(\text{SiH}_4 + \text{NH}_3)$ during the plasma-enhanced chemical vapor deposition (PECVD) process. The effects of R ratio on the material's composition, crystallinity, surface passivation, and contact resistivity are investigated. The poly-SiN_x contact exhibits improved surface passivation in comparison with the reference poly-Si without N incorporation. The best double-sided passivated n-type alkaline-polished crystalline silicon wafer with the n-poly-SiN_x/SiO_x manifests the highest implied open-circuit voltage (iV_{oc}) of ≈ 745 mV, with the corresponding single-sided saturated current density of 1.7 fA cm^{-2} and the effective lifetime (τ_{eff}) of 10 ms at the injection level of $\approx 1 \times 10^{15} \text{ cm}^{-3}$. In contrast, the controlled sample with an n-poly-Si/SiO_x passivation contact has a maximal iV_{oc} of 738 mV.

However, the primary drawback of the N doping is to raise the contact resistivity, but which is still in an acceptable range and shows little effect on the performance of solar cell with full-area contact. The proof-of-concept TOPCon solar cell using the n-poly-SiN_x/SiO_x passivating contact has achieved an efficiency of 23.88%, indicating the potential of the n-poly-SiN_x for high-efficiency TOPCon solar cells.

1. Introduction

The passivated contact technology with polysilicon (poly-Si) and ultrathin silicon oxide (SiO_x), also named as tunnel oxide passivated contact (TOPCon), polysilicon on oxide (POLO),^[1] industrial-TOPCon (iTOPCon),^[2] and MonoPoly,^[3] has attracted tremendous attentions since 2013.^[4] With the great efforts of the photovoltaic community, the champion efficiencies of n-type and p-type solar cells with the TOPCon technology have been promoted to 25.8% and 26.1%, respectively,^[5,6] which are higher than the mainstream passivated emitter and rear contact (PERC) cells. More importantly, the TOPCon technology displays an excellent compatibility with the PERC solar cell production line^[2] and high efficiency for mass production cell technology, which will help to upgrade the PERC mass production lines in the future.


The efficiency improvement of TOPCon cells verse PERC cells is attributed to the excellent rear passivation quality by the

Q. Yang, Z. Liu, Y. Lin, W. Liu, M. Liao, M. Feng, Y. Zhi, J. Zheng, L. Lu, D. Ma, Q. Han, H. Cheng, Z. Yang, Y. Zeng, B. Yan, J. Ye
Institute of New Energy Technology
Ningbo Institute of Materials Technology and Engineering
Chinese Academy of Sciences (CAS)
Ningbo City 315201, P. R. China
E-mail: yuhengzeng@nimte.ac.cn; yanbaojie@nimte.ac.cn;
jichun.ye@nimte.ac.cn

Q. Yang, Z. Liu
College of Materials Science and Opto-Electronic Technology
University of Chinese Academy of Sciences
Beijing City 100049, P. R. China

Q. Yang, K. Ding, W. Duan
IEK5-Photovoltaics
Forschungszentrum Jülich
52425 Jülich, Germany

H. Chen, Y. Wang
Suzhou Tuosheng Intelligent Equipment Co., Ltd
Suzhou City, Jiangsu Province 215156, P. R. China

 The ORCID identification number(s) for the author(s) of this article can be found under <https://doi.org/10.1002/solr.202100644>.

DOI: 10.1002/solr.202100644

chemical-effect passivation from the ultrathin SiO_x layer and the hydrogen atoms and by the field-effect passivation from the heavily doped poly-Si layer.^[7] The optimal passivation quality of phosphorous (P)-doped poly-Si (n-poly-Si) and ultrathin SiO_x -coated n-type c-Si wafer (lifetime sample) has realized an implied open-circuit voltage (iV_{oc}) of >745 mV and a saturated recombination current density (J_0) of $<1.5 \text{ fA cm}^{-1}$.^[1,2,8,9] The microstructure and optoelectronic properties of the poly-Si film is of great importance for passivation quality.^[10–12] In our previous work, we found that the P-doped polycrystalline silicon-carbide (n-poly-SiC_x) film can improve the passivation quality of bifacial TOPCon lifetime samples, manifesting the champion iV_{oc} of 750 mV,^[13] much better than the counterpart with the carbon-free n-poly-Si. We found that one of the primary reasons of improving passivation is that the carbon incorporation suppresses the crystallization of polysilicon films and thus reduces the probability of blistering.^[13] A reasonable speculation is that nitrogen (N) incorporation would have the similar potential of suppressing the blistering, which is mainly attributed to the reduction of interface by suppressing the crystallization of polysilicon and serving as the stress-release paths, such as the carbon doping case.^[13] Therefore, it is interesting to investigate the effects of polycrystalline silicon-nitride (poly-SiN_x) passivated contact and its potential application for high efficiency TOPCon solar cells. However, to the best of our knowledge, there

is still no work reporting the effects of N-incorporation on TOPCon passivation quality and solar cell performance.

In this contribution, we explore the possibility of applying P-doped poly-SiN_x to TOPCon solar cells, including the effects of nitrogen incorporation in the polycrystalline alloy film on the passivation quality and contact resistivity. The P-doped poly-SiN_x films are fabricated using plasma-enhanced chemical vapor deposition (PECVD) and thermal annealing at high temperature. The incorporation of nitrogen is through adding NH_3 gas into the SiH_4 -based plasma and the nitrogen concentration is controlled by adjusting the $\text{NH}_3/(\text{SiH}_4 + \text{NH}_3)$ gas flow ratio (R). It is found that the passivation quality and contact resistivity of the P-doped n-type poly-SiN_x contact are highly related to the R value and the crystallization temperature. Finally, we demonstrate a 23.88% high-efficiency n-type solar cell using the n-type poly-SiN_x as the rear surface passivation contact, showing the potential of P-doped poly-SiN_x for practical application.

2. Results and Discussion

We first study the incorporation of nitrogen as a function of R ranging from 0.25 to 0.75 using X-ray photoelectron spectroscopy (XPS) measurements on the 820°C -annealed hydrogenated silicon-nitride ($\text{a-SiN}_x\text{:H}$) thin films with phosphorous doping. The

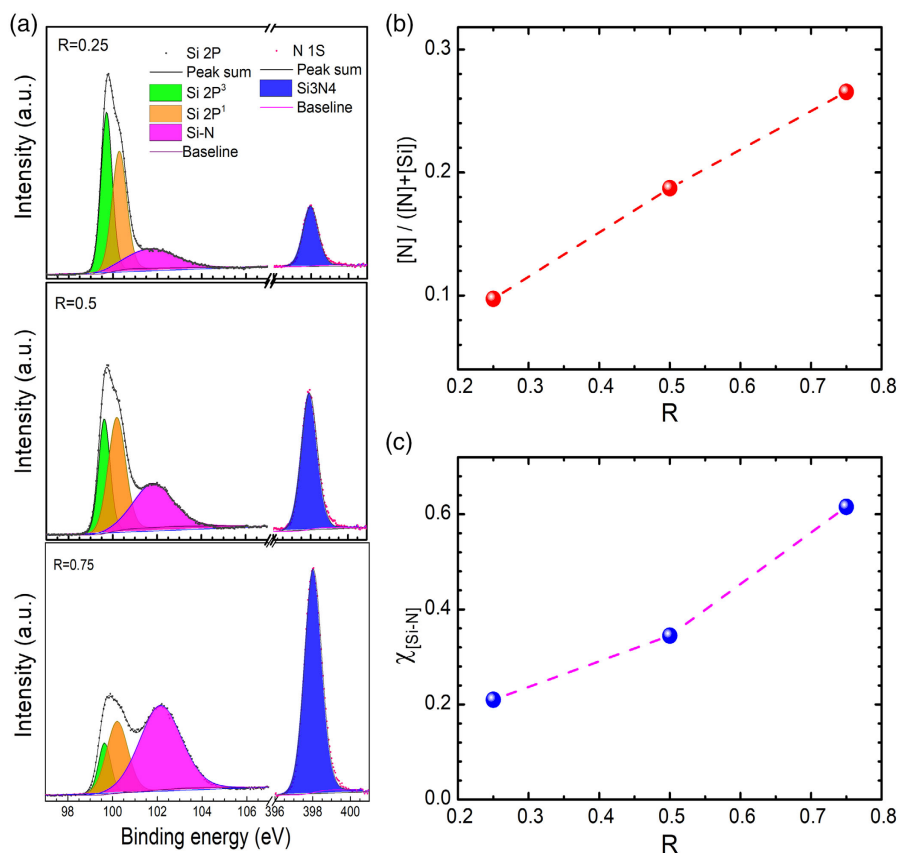


Figure 1. a) XPS spectra of Si 2p and N 1s for the $R=0.25, 0.5$, and 0.75 of the 820°C -annealed P-doped poly-SiN_x samples. b) The approximate proportion of N concentration and c) the proportion of Si atoms bonded with N ($\text{Si}^{3/4+}$) as a function of R values.

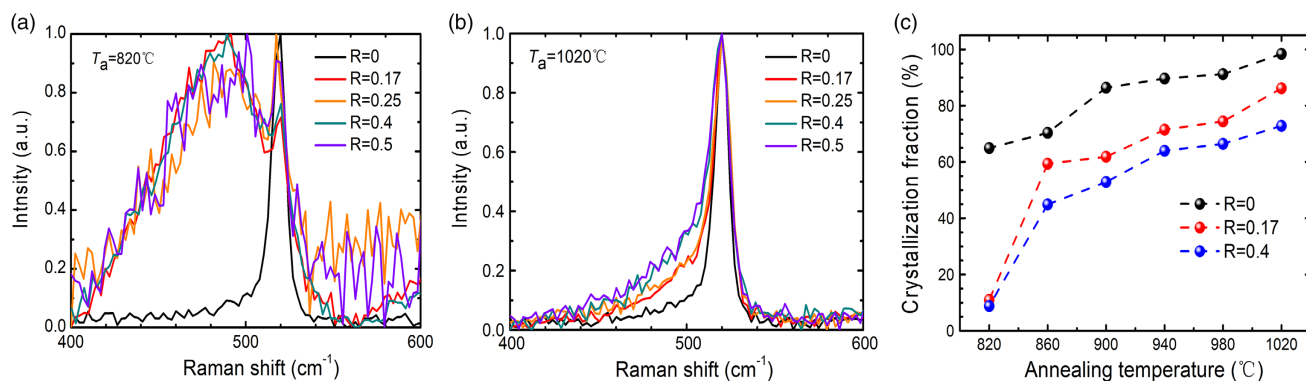


Figure 2. Raman spectra for the samples with various R values annealed at a) 820 °C and b) 1020 °C, c) the crystallinity of three sets of samples with $R = 0, 0.17$, and 0.4 as the function of annealing temperature in the range from 820 to 1020 °C.

proportion of N 1s peak represents the incorporation of nitrogen into the poly-SiN_x. As shown in Figure 1a, it is confirmed that nitrogen is induced into the film effectively by using NH₃ as the nitrogen source. It is intuitively seen that with the increase in R value, the peak signal intensity related to N increases. Furthermore, using Equation (1) can estimate the nitrogen concentration in the film.

$$\chi_{[N]} = \frac{\frac{I_{N1s}}{RSF(N)}}{\frac{I_{N1s}}{RSF(N)} + \frac{I_{Si2p}}{RSF(Si)}} \quad (1)$$

where I_{N1s} and I_{Si2p} are the integral area of N 1s and Si 2p peaks of the XPS spectra, respectively; RSF is the relative sensitivity factor, which is 1.8 for N and 0.817 for Si. In addition, I_{Si2p} can be divided into I_{Si2p3} , I_{Si2p1} , and I_{Si-N} , with the corresponding peak positions at 99.8, 100.4, and 102.0 eV. In addition, the I_{N1s} , I_{Si3N4} , has a peak position of 397.6 eV. It is observed that the nitrogen content is increased with the R value, as shown in Figure 1b. It is found that the nitrogen concentration has reached ≈ 9.7 at% with the R value of 0.25 and grows to ≈ 26 at% with the R value of 0.75. A roughly linear trend between the nitrogen content and the R value is observed with a slope of 0.33 in the R range of 0.25–0.75, which is consistent with reported in the literature.^[14] Although the XPS measurement is only a coarse estimation of the nitrogen concentration, the measurement results may still conclude that nitrogen is incorporated into amorphous silicon based thin film effectively by PECVD deposition. Figure 1c shows the proportion of Si atoms bonding with N, and its calculation is made by using Equation (2).

$$\chi_{[Si-N]} = \frac{I_{Si-N}}{I_{Si2p3} + I_{Si2p1} + I_{Si-N}} \quad (2)$$

The result in Figure 1c shows that the percentage of nitration Si^{3+/4+} atoms (Si–N) bonded with N atoms increases with the increase in the R value, and the percentage values are $\approx 21\%$, $\approx 32\%$, and 62% with the R values of 0.25, 0.5, and 0.75, respectively. It confirms that the incorporated nitrogen atoms are bonded with Si atoms and prove a significant amount of nitration in the silicon-based films.

A thermal treatment is used to crystallize the P-doped a-SiN_x:H films and activate the phosphorus impurity. In details, the P-doped

a-SiN_x films are annealed at the temperatures ranging from 820 to 1020 °C to form n-type poly-SiN_x, whose crystallinity is analyzed by using a 325 nm UV Raman spectroscopy. The Raman spectra of the annealed samples at 820 °C with various R values are shown in Figure 2a. It is found that the sample made with no NH₃ flow shows a spectrum with full crystallization with a sharp c-Si peak at 520 cm⁻¹, while the samples with nonzero R values all present the signature of amorphous phase with a broad peak at 480 cm⁻¹, which implies that the incorporation of nitrogen hinders the crystallization significantly. As shown in Figure 2b, raising the annealing temperature to 1020 °C, all of the samples exhibit the sharp peak at 520 cm⁻¹ with a tail in the low wave number side, indicating a mixed phase structure of crystalline and amorphous phases. It appears that the component of low energy tail increases with the increase in R value. To investigate the crystallinity quantitatively, the Raman spectra are decomposed with three peaks at approximately at 480, 510, and 520 cm⁻¹ for the amorphous, grain boundary, and crystalline phases, respectively. The crystallinity is defined by the integrated area ratio of grain boundary and crystalline phases over the total area of the three peaks. Figure 2c shows the effects of nitrogen concentration and annealing temperature on the crystallinity. As can be seen, the P-doped a-SiN_x samples start to be crystallized at the annealing temperature of 860 °C and the crystallinity increases with the increase in annealing temperature. Generally speaking, the samples with a higher nitrogen content requires a higher annealing temperature to reach a similar crystallinity, which agrees with the as-known phenomenon.^[15] The crystallinity of the P-doped poly-SiN_x subjected to 900 °C annealing is high enough for solar cell application. As an example, the crystallinity values are $\approx 60\%$ and $\approx 50\%$ for the R values of 0.17 and 0.4, respectively.

The effects of R value and annealing temperature on the passivation quality of the double side n-poly-SiN_x/SiO_x passivated samples were investigated at the as-annealed state and the hydrogenated state with an AlO_x:H capping layer, respectively, as shown in Figures 3b, and the structure of lifetime sample is shown in Figures 3a. The observations are presented as follows: 1) the annealing temperature influences the passivation quality significantly. In the as-annealed state, the iV_{oc} of the samples annealed at 860–940 °C keeps a high level of 710–730 mV for

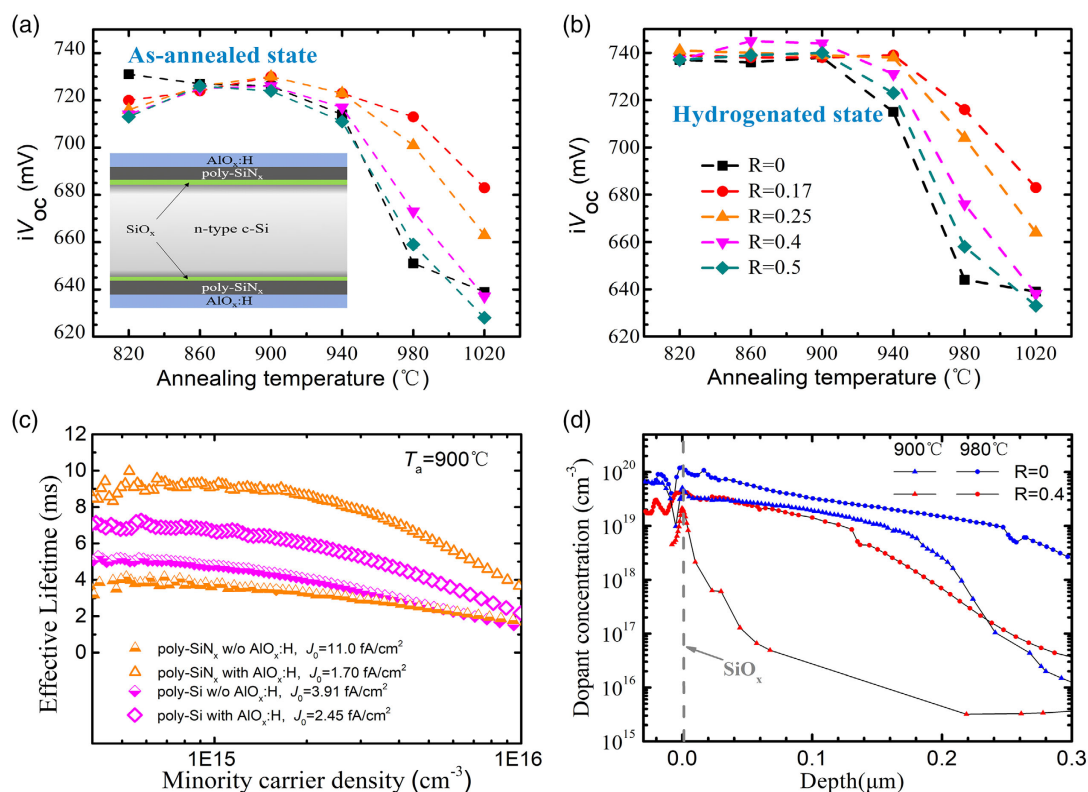


Figure 3. a,b) iV_{oc} of the samples with different R value as a function of annealing temperature in the as-annealed state and the hydrogenated state with $AlO_x:H$ capping layer. The insert is the structure of lifetime sample covered by AlO_x -capping layer. c) Effective lifetimes (τ_{eff}) of the samples with $R = 0$ and 0.4 annealed at $900^\circ C$. d) The P profiles of the 900 and $980^\circ C$ -annealed $poly-Si$ and $poly-SiN_x$ ($R = 0.4$) passivating samples.

most of the samples. However, the iV_{oc} drops severely when the annealing temperature increases to higher than $980^\circ C$. The passivation quality becomes poor after the $1020^\circ C$ annealing. 2) The nitrogen concentration as measured with the R value exerts clear effects on the passivation quality and the optimized annealing temperature. For the as-annealed samples without nitrogen incorporation ($R = 0$), the passivation quality decays monotonously as the increase in annealing temperature from 820 to $1020^\circ C$. In contrast, for the as-annealed samples with the given R values, the optimal passivation quality appears in the temperature range of 860 – $900^\circ C$, while the passivation quality starts to decay when the temperature increases to higher than $940^\circ C$. However, the relationship between the optimal iV_{oc} and optimized annealing temperature is not highly related to the nitrogen concentration. In general, the P-doped $poly-SiN_x$ passivated contact with $R = 0.17$ – 0.25 shows an improved passivation quality as the temperature over $940^\circ C$, but further increasing the R value degrades the passivation quality. The degradation of passivation with $R \geq 0.4$ may be caused by extending defects or weakening the field passivation relative to high-concentration N doping, which requires further investigation. 3) The $AlO_x:H$ hydrogenation improves the passivation quality, which is presumably caused by introducing H atoms to interface and passivating the dangling bonds. The $AlO_x:H$ hydrogenation promotes most of the iV_{oc} s to ≈ 735 – 740 mV in the case of the annealing temperature higher than $900^\circ C$. However, the effects of $AlO_x:H$

hydrogenation for the samples annealed at the temperature higher than $980^\circ C$ are limited, which is likely due to the highly destroyed interfacial SiO_x and the significant P-diffusion induced Auger recombination during such high-temperature annealing. The best iV_{oc} and single-sided J_0 reach 745 mV and 1.7 fA cm^{-2} in the $AlO_x:H$ hydrogenated sample with $R = 0.4$ annealed at 860 – $900^\circ C$. Correspondingly, the τ_{eff} of the same sample reaches ≈ 10 ms at the injection level of $< 1 \times 10^{15} cm^{-3}$, as shown in Figures 3c, which is higher than the counterpart samples without nitrogen incorporation, whose iV_{oc} is 738 mV and τ_{eff} is ≈ 7 ms. 4) The typical ECV profiles of the 900 and $980^\circ C$ -annealed $poly-Si$ and $poly-SiN_x$ ($R = 0.4$) samples are shown in Figure 3d. As can be seen, the P impurity has been activated and diffused into Si substrate in the 900 and $980^\circ C$ -annealed $poly-Si$ sample. In contrast, the activated P concentrations in the $900^\circ C$ -annealed $poly-SiN_x$ is only $\approx 1 \times 10^{19} cm^{-3}$, and it raises to 2 – $3 \times 10^{19} cm^{-3}$. Moreover, the in-diffusion P profiles in the $poly-SiN_x$ samples become much shallower than that in the $poly-Si$ one. The ECV measurements indicate that N doping retards the activation and in-diffusion of P, which will degrade the contact performance and weaken the field-effect passivation. Thus, to optimize the N doping and annealing temperature is necessary for a high-efficiency device.

To evaluate the contact properties of P-doped $poly-SiN_x$ contact for device application, the Cox–Strack (CS) method is used to estimate the contact resistivity (ρ_c). The test structure for CS measurement is referred to the inset of Figure 4a. The dot-shaped Ag

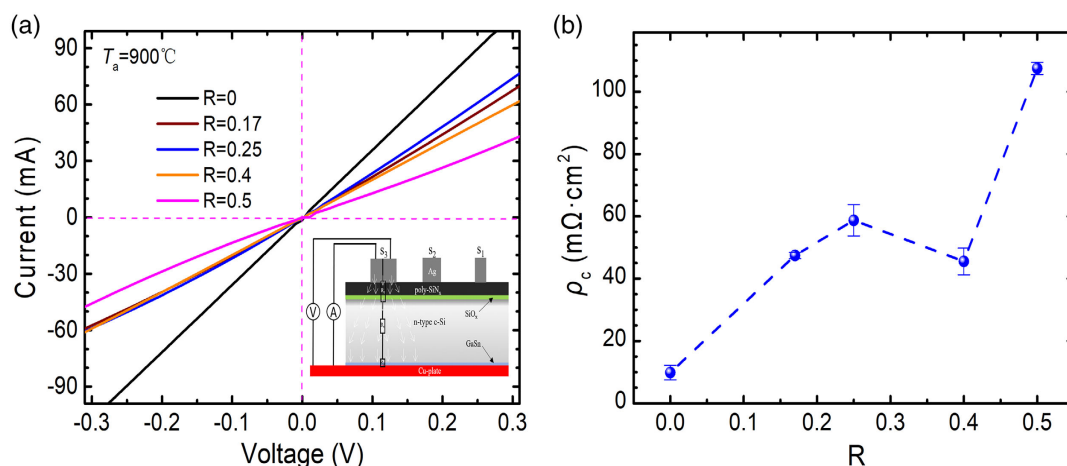


Figure 4. a) Dark I - V curves of samples with different R values annealed at 900°C . The inset is the test structure using the CS method. b) Contact resistivity of the 900°C -annealed samples with different R values.

electrodes with different diameters are deposited on the annealed poly- SiN_x and full area contact on the other side of the c-Si wafer. Generally, the current-voltage (I - V) curves of the 900°C -annealed samples with R value ranging from 0 to 0.5 manifest a clear Ohmic-contact feature, as shown in Figure 4a. Moreover,

the ρ_c values of the samples with different R values are extracted and the results are shown Figure 4b. The N-free poly-Si passivating contact shows a low ρ_c of $\approx 5 \text{ m}\Omega \text{ cm}^2$. However, the incorporation of nitrogen leads to a significant increase of ρ_c , i.e., the ρ_c is increased to $\approx 100 \text{ m}\Omega \text{ cm}^2$ with $R = 0.5$. Note that the ρ_c is

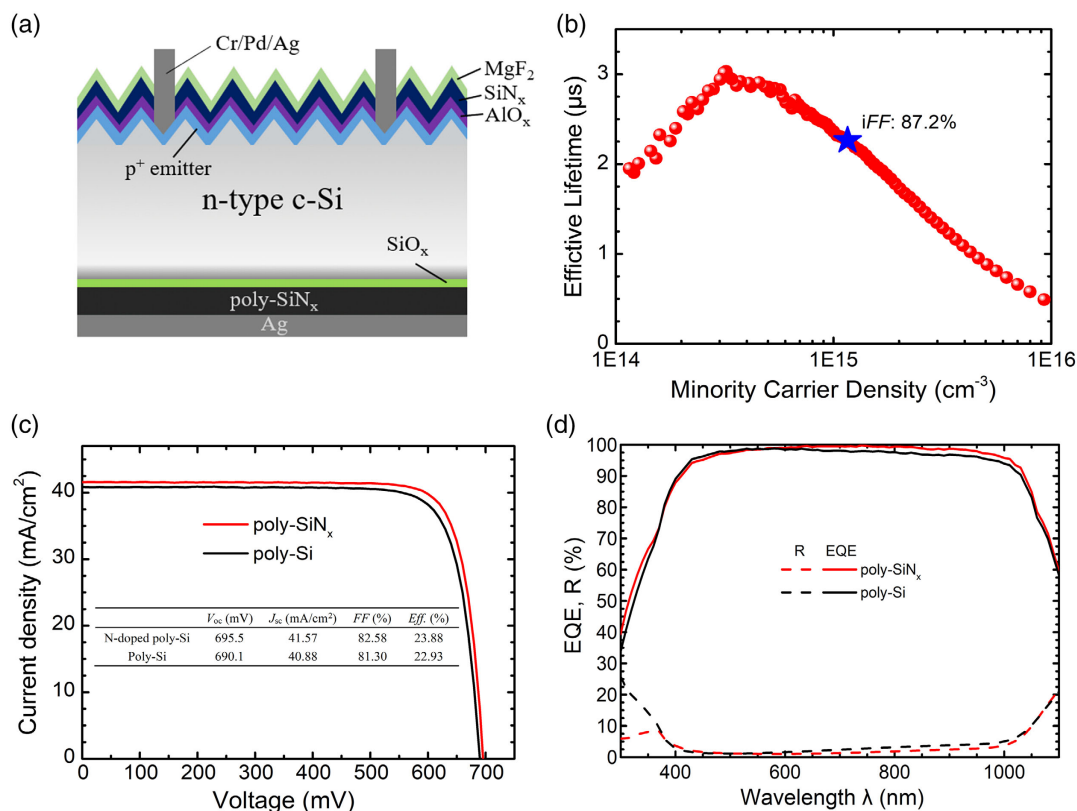


Figure 5. a) Schematic of the n-type TOPCon solar cell with a rear full-area electrode. b) Effective lifetime as a function of minority carrier density in a quasisolar cell with the P-doped poly- SiN_x rear contact, featuring an excellent iFF of 87.2%. c) Illumination J - V curves two solar cells with the P-doped poly- SiN_x and poly-Si rear contact; the inset table lists the performance parameters of the solar cells ($2 \times 2 \text{ cm}$). d) EQE and reflectance (R) of the two solar cells.

around $50 \text{ m}\Omega \text{ cm}^2$ at $R = 0.17\text{--}0.4$, which might not be a serious problem for a TOPCon solar cell with a full rear electrode. Moreover, the slightly lower ρ_c at $R = 0.4$ is possibly attributed to the experimental error, as the tendency is that the higher the R value, the lower is the activation and the weaker is the P diffusion into the c-Si wafer.

To examine the potential of P-doped poly-SiN_x-passivated contact in the application for high-efficiency TOPCon solar cells, we used the 900 °C-annealed P-doped poly-SiN_x with the R value of 0.4 to serve as the full-area rear contact, whose device structure is shown in **Figure 5a**. Before the fabrication of complete cells, the quality of the semifinished (quasi-) solar cells without the front and rear electrodes manifests an excellent passivation quality, i.e., the statistical average iV_{oc} is over 720 mV and the total saturation current density ($J_{0, \text{total}}$) is below 25 fA cm^{-2} . The champion iV_{oc} of the quasisolar cell reaches 724 mV with an excellent implied fill factor (iFF) of 87.2%, indicating the potential to fabricate a high efficiency solar cell. **Figure 5b** shows effective lifetime curve of the quasisolar cell, with its iFF marked.

The champion efficiency of the solar cell with the P-doped poly-SiN_x/SiO_x rear contact is 23.88%, with an open-circuit voltage (V_{oc}) of 695.5 mV, a short-circuit current (J_{sc}) of 41.57 mA cm^{-2} , and an FF of 82.58%. The controlled solar cell with the P-doped poly-Si shows the best efficiency of 22.93%, with a V_{oc} of 690.1 mV, a J_{sc} of 40.88 mA cm^{-2} , and an FF of 81.30%. The illuminated J - V curves of the two cells are plotted in **Figure 5c**. Moreover, the external quantum efficiency (EQE) and reflectance (R) curves of the two cells are shown in **Figure 5d**, indicating that the device with the P-doped poly-SiN_x contact shows an improved EQE response in the wavelength range from ≈ 600 to 1200 nm in comparison with the counterpart with the P-doped poly-Si contact. The gain of J_{sc} possibly results from the better rear passivation quality and less parasitic absorption in the rear P-doped poly-SiN_x layer.

3. Conclusion

In this work, we report the P-doped poly-SiN_x/SiO_x tunnel-passivated contact for high-efficiency TOPCon solar cells. The nitrogen content is controlled by the $R = \text{NH}_3/(\text{SiH}_4 + \text{NH}_3)$ gas ratio in the PECVD process. We conduct a systematical study on the effects of the R value and annealing temperature on the composition, crystallinity, passivation quality, and contact resistivity. The main observations are listed as follows. 1) Nitrogen is easily to introduce into the film and further to form a-SiN_x:H film, which can be crystallized into poly-SiN_x after high-temperature annealing. The incorporation of nitrogen hinders the crystallization, as well as the activation and in-diffusion of phosphorus, and therefore a higher annealing temperature is required for a sample with a higher nitrogen content to form the same polycrystalline structure. 2) The nitrogen incorporation shows a positive effect on the passivation quality, i.e., the statistical iV_{oc} maintains ≈ 740 mV after the hydrogenation, and the champion iV_{oc} of ≈ 745 mV ($R = 0.4$ and 860–900 °C annealing) with the single-sided J_0 of 1.7 fA cm^{-2} and τ_{eff} of ≈ 10 ms has been achieved, which is better than the control sample with the poly-Si without intentional nitrogen incorporation. 3) The primary drawback is that the nitrogen incorporation raises the ρ_c , which requires a careful balance between the ρ_c and other

properties, such as the passivation quality and optical parasitic absorption. Finally, the proof-of-concept n-type TOPCon solar cells using the full-area rear P-doped poly-SiN_x contact achieves an efficiency of 23.88%, indicating the potential of applying the P-doped poly-SiN_x layer in high-efficiency TOPCon solar cells.

4. Experimental Section

Lifetime and Suns-Voc Samples: The 1–3 $\Omega \text{ cm}$, <100>-oriented n-type Czochralski (CZ) silicon wafers with a thickness of 170 μm were used as the substrates for lifetime samples. After a standard RCA cleaning and a diluted HF dip, an ultrathin SiO_x layer was grown by oxidation in a nitric acid bath (68 wt% HNO₃) at 110 °C for 15 min, which was the so-called NAOS SiO_x. Subsequently, a 30–40 nm-thick phosphorus-doped a-SiN_x:H layer was deposited on both sides of the c-Si substrate using a 13.56 MHz PECVD system with SiH₄, PH₃, NH₃, and H₂ as the reaction gases. The nitrogen content was controlled by the gas flow ratio (R) of NH₃ to (SiH₄ + NH₃). Then, the samples were thermally annealed at the temperature in the range from 820 to 1020 °C for 30 min within a N₂ protective atmosphere in a quartz tube furnace. Finally, the as-annealed samples were capped by atomic layer deposition (ALD)-grown AlO_x:H and subjected to a 450 °C annealing to activate the AlO_x:H hydrogenation.

The lifetime of samples was measured using a Sinton (WCT-120) system and the single-side saturated current density (J_0) and implied open-circuit voltage (iV_{oc}) were extracted from the measured photoconductive decays with the transient mode (T mode). The nitrogen content was measured using an XPS (AXIS ULTRA DLD). The crystallinity of the P-doped poly-SiN_x was measured using a Raman spectroscopy with a 325 nm laser as the excitation source (Renishaw inVia-reflex).^[16] The contact resistivity was measured using the CS method by depositing circular-dot Ag electrodes with different diameters on the top surface of the poly-SiN_x layer. The sheet resistance (R_{sh}) was measured with four point probe meter (FPP).

Solar Cells: The 2 cm \times 2 cm solar cells using the P-doped poly-SiN_x on the rear side were fabricated on <100>-oriented n-type CZ wafers with a resistivity of $\approx 1 \Omega \text{ cm}$. The texture surface was formed by chemical etching in a KOH solution. The front-side boron-doped emitter was prepared through BBr₃ diffusion, and then the rear surface was polished by alkaline to remove the wrap-round deposited boron diffusion zone. The rear-side ultrathin SiO_x layer was prepared in HNO₃ bath (NAOS) or plasma-assisted N₂O oxidation (PANO)^[8] after RCA cleaning and HF dip. A phosphorous-doped a-SiN_x:H layer with a thickness of ≈ 30 nm was deposited with PECVD on the SiO_x. Subsequently, the sample was annealed at 900 °C for 30 min for preparing the P-doped poly-SiN_x and activating the phosphorus doping. Note that the optimal annealing temperatures at 900 °C were similar for the N-free poly-Si passivating contact with PANO SiO_x^[8] and for the N-alloyed one with NAOS SiO_x. The front-side boron-diffused emitter was passivated by ALD-deposited AlO_x and PECVD-deposited SiN_x stack layers. The pattern of the front electrode with a line width of $6 \pm 1 \mu\text{m}$ was defined through photolithography. The Cr/Pd/Ag seed layer was deposited with electron-beam evaporation and was thickened to $\approx 5 \mu\text{m}$ with electroplating. The rear side was covered by a full-area Ag electrode deposited by thermal evaporation. Finally, an MgF₂ layer was deposited with thermal evaporation on the front side to enhance antireflectance. The solar cell performance was characterized using a Suns-V_{oc} analysis system (Sinton WTC-120) and a solar simulator (Enlitech, SS-F5-3A) under AM1.5 illumination (100 mW cm^{-2}) at 25 °C. Finally, the EQE of solar cell was measured using EQE system (Enlitech, QE-R3011).

Acknowledgements

Q.Y. and Z.L. contributed equally to this work. This work was supported by the National Natural Science Foundation of China (grant nos. 61974178, 61874177, and 62004199), the Ningbo "Innovation 2025" Major Project (grant no. 2020Z098), the Key Research and Development Program of

Zhejiang Province (grant no. 2021C01006), the National Key R&D Program of China (grant no. 2018YFB1500403), the Zhejiang Energy Group (Project No. znkj-2018-118), the Youth Innovation Promotion Association (2018333), the Zhejiang Provincial Natural Science Foundation (LY19F040002).

Conflict of Interest

The authors declare no conflict of interest.

Data Availability Statement

The data that support the findings of this study are available from the corresponding authors upon reasonable request.

Keywords

passivating contacts, plasma-enhanced chemical vapor deposition, polycrystalline silicon nitride, TOPCon

Received: August 14, 2021

Revised: September 8, 2021

Published online: September 20, 2021

- [1] R. Peibst, Y. Larionova, S. Reiter, M. Turcu, R. Brendel, D. Tetzlaff, J. Krügener, T. Wietler, U. Höhne, J.-D. Kähler, H. Mehlich, S. Frigge, in *EU PVSEC 2016-32nd European Photovoltaic Solar Energy Conf. and Exhibition*, Munich, Germany **2016**.
- [2] Y. Chen, D. Chen, C. Liu, W. Zigang, Y. Zou, Y. He, Y. Wang, L. Yuan, J. Gong, W. Lin, X. Zhang, Y. Yang, H. Shen, Z. Feng, P. P. Altermatt, P. J. Verlinden, *Prog. Photovoltaics* **2019**, 27, 827.
- [3] N. Nandakumar, J. Rodriguez, T. Kluge, T. Große, L. Fondop, P. Padhamnath, N. Balaji, M. König, S. Duttgupta, *Prog. Photovoltaics* **2019**, 27, 107.
- [4] F. Feldmann, M. Bivour, C. Reichel, M. Hermle, S. W. Glunz, in *Proc. of the 28th EUPVSEC*, Paris, France, **2013**, p. 988.
- [5] A. Richter, J. Benick, F. Feldmann, A. Fell, M. Hermle, S. W. Glunz, *Sol. Energy Mater. Sol. Cells* **2017**, 173, 96.
- [6] F. Haase, C. Hollemann, S. Schäfer, A. Merkle, M. Rienäcker, J. Krügener, R. Brendel, R. Peibst, *Sol. Energy Mater. Sol. Cells* **2018**, 186, 184.
- [7] R. Brendel, R. Peibst, *IEEE J. Photovoltaics* **2016**, 6, 1413.
- [8] Y. Huang, M. Liao, Z. Wang, X. Guo, C. Jiang, Q. Yang, D. Huang, Z. Yuan, J. Yang, X. Zhang, Q. Wang, H. Jin, W. Guo, J. Sheng, M. Al-Jassim, C. Shou, Y. Zeng, B. Yan, J. Ye, *Sol. Energy Mater. Sol. Cells* **2020**, 208, 110389.
- [9] Z. Rui, Y. Zeng, X. Guo, Q. Yang, Z. Wang, C. Shou, W. Ding, J. Yang, X. Zhang, Q. Wang, H. Jin, M. Liao, S. Huang, B. Yan, J. Ye, *Sol. Energy* **2019**, 194, 18.
- [10] A. Morisset, R. Cabal, B. Grange, C. Marchat, J. Alvarez, M.-E. Gueunier-Farret, S. Dubois, J.-P. Kleider, *Sol. Energy Mater. Sol. Cells* **2019**, 200, 109912.
- [11] Y. Tao, E. L. Chang, A. Upadhyaya, B. Roundaville, Y.-W. Ok, K. Madani, C.-W. Chen, K. Tate, V. Upadhyaya, F. Zimbardi, in *42nd IEEE Photovoltaic Specialist Conference, PVSC 2015*, New Orleans, USA **2015**, p. 1.
- [12] T. Gao, Q. Yang, X. Guo, Y. Huang, Z. Zhang, Z. Wang, M. Liao, C. Shou, Y. Zeng, B. Yan, G. Hou, X. Zhang, Y. Zhao, J. Ye, *Sol. Energy Mater. Sol. Cells* **2019**, 200, 109926.
- [13] Y. Lin, Z. Yang, Z. Liu, J. Zheng, M. Feng, Y. Zhi, L. Lu, M. Liao, W. Liu, D. Ma, Q. Han, H. Cheng, Q. Zeng, Z. Yuan, B. Yan, Y. Zeng, J. Ye, *Dual-Functional Carbon-Doped Polysilicon Films for Passivating Contact Solar Cells: Regulating Physical Contacts while Promoting Photoelectrical Properties*, submitted to *Journal*, under review, **2021**.
- [14] A. Ingenito, G. Nogay, J. Stuckelberger, P. Wyss, L. Gnocchi, C. Allebe, J. Horzel, M. Despeisse, F.-J. Haug, P. Löper, C. Ballif, *IEEE J. Photovoltaics* **2018**, 9, 346.
- [15] A. Morimoto, T. Kataoka, M. Kumeda, T. Shimizu, *Philos. Mag. B* **1984**, 50, 517.
- [16] Y. Huang, Y. Zeng, Z. Zhang, X. Guo, M. Liao, C. Shou, S. Huang, B. Yan, J. Ye, *Sol. Energy Mater. Sol. Cells* **2019**, 192, 154.